Interactions of Magnetic Particles in a Rotational Magnetic Field

A. Weddemann*, A. Auge, F. Wittbracht, S. Herth, A. Hütten
Bielefeld University, Department of Physics
*Universitätsstr. 25, 33615 Bielefeld, weddeman@physik.uni-bielefeld.de

Abstract: Particle-particle interactions are usually neglected when considering the behaviour of magnetic particles so called magnetic beads in e.g. a microfluidic device. However, if the particle density exceeds a critical limit, this assumption might not lead to proper results anymore. In this paper the particle-particle interaction of magnetic beads in an external magnetic field will be discussed. It is shown that the magnetic force acting on the particles will lead to very high particle velocities. Therefore, apart from the magnetic interaction, their fluidic forces are also of concern. These two contributions will be compared.
Because of high local Reynolds numbers close to the particles a very fine local mesh is needed. The mesh deformation due to the particle movement is described within an ALE-framework with the help of a second domain triangulation using linear finite element shape functions.

Keywords: ALE-methods, second domain triangulation, magnetic particles

1. Introduction

Predicting the behaviour of magnetic particles in microfluidic systems (e.g. lab-on-a-chip-systems) an often made simplifying assumption is that particle-particle interaction can be neglectted [1,2]. Experimentally, this can be easily achieved by working with low concentrations. However, this constraint will lead to longer time scales for applications, whereas it cannot be assured that there are no areas where particles cluster together to higher concentrations. Therefore, it is also interesting to study the behaviour of systems, where the assumption of low concentration does not hold.

In order to make proper predictions on particle behaviour in highly concentrated dilutions, we will investigate a system of superparamagnetic particles in an external field, moving because of their magnetic interactions as well as particle-fluid interactions.

2. Governing equations

The investigated particles are supposed to be superparamagnetic, i.e. the magnetization of the particles is aligned with the external field. In particular, we will restrict our analysis to single-domain spherical particles. Therefore, we may write the resulting particle stray field as a function of the external magnetic field $\boldsymbol{B}_{ex}$. The stray field $\boldsymbol{B}$ of a sphere with radius R can be written as [3]:

$$\boldsymbol{B} = -\mu_0 \nabla \Phi \qquad (2.1)$$

with $\Phi(\boldsymbol{r}) = \frac{1}{3} M_s r \cos\theta$,

where $r = |\boldsymbol{r}|$, $\theta = \sphericalangle(\boldsymbol{r}, \boldsymbol{B}_{ex})$ and M_s denotes the saturation magnetization of the particle material. The particle magnetization $\boldsymbol{M}_i$ of the i-th particle P_i will be influenced by the stray field $\boldsymbol{B}_j$ of other beads. Particularly, a torque $\boldsymbol{\tau}_i$ and a force $\boldsymbol{F}_{mag,i}$ is exerted. These are given by the following integrals taken over the whole particle domain

$$\tau_i = \sum_{j \neq i} \int_{P_i} \boldsymbol{M}_i \times \boldsymbol{B}_j \, dx \qquad (2.2)$$

and $$\boldsymbol{F}_{i,mag} = \sum_{j \neq i} \int_{P_i} (\boldsymbol{M}_i \cdot \nabla) \boldsymbol{B}_j \, dx \,. \qquad (2.3)$$

The force acting on the particles results in the motion of the beads. From a hydrodynamic point of view the particle boundaries can be regarded as moving “walls”, where a common assumption for the velocity is, that the liquid directly located to these, moves with the velocity of the wall itself (no-slip-condition). Therefore, the particle movement will induce a fluid flow nearby, influencing further particles. Thus, the behaviour of the fluid has to be discussed as well.
Commonly, it is sufficient to discuss the linearized Stokes-Equation to describe the fluid behaviour on the micro- or nanoscale. However, as we will see, in the particular case, full Navier-Stokes equations have to be considered, i.e. the

equation of continuity representing the conservation of mass

$$\nabla \cdot \boldsymbol{u} = 0\,, \tag{2.4}$$

where $\boldsymbol{u}$ is the velocity field, and the Navier-Stokes equation, the equation of momentum conservation

$$\frac{\partial \boldsymbol{u}}{\partial t} + (\boldsymbol{u} \cdot \nabla)\boldsymbol{u} = -\frac{\nabla p}{\rho} + \frac{\eta}{\rho}\Delta \boldsymbol{u} + \boldsymbol{f}\,. \tag{2.5}$$

Here p denotes the pressure field, η and ρ are the viscosity and the density of the fluid, respectively, and $\boldsymbol{f}$ is the force density acting on the liquid, i.e. the force from the particles. With the values of $\boldsymbol{B}$, $\boldsymbol{u}$ and p the motion of the particles can be derived from the following system of ordinary differential equations

$$m_i \frac{d\boldsymbol{a}_i}{dt} = \boldsymbol{F}_{i,fluid} + \boldsymbol{F}_{i,mag} + \boldsymbol{F}_{i,pen} \tag{2.6}$$

By the index i, we indicate the i-th particle, where the following assignments are used

m_i	mass of i-th particle
$\boldsymbol{F}_{i,fluid}$	fluidic forces acting on i-th particle
$\boldsymbol{F}_{i,mag}$	magnetic forces acting on i-th particle
$\boldsymbol{F}_{i,pen}$	penality forces acting on i-th particle, preventing particles from overlapping

As the Reynolds number can reach high local values we cannot use Stokes drag law for $\boldsymbol{F}_{i,fluid}$, but have to apply the more general Khan-Richardson force [4]

$$\boldsymbol{F}_{i,fluid} = \pi r^2 (\boldsymbol{u} - \boldsymbol{v})^2 \cdot (1.84 Re_p^{-0.31} + 0.293 Re_p^{0.06})^{3.45} \tag{2.7}$$

with $\quad Re_p = \dfrac{2r\rho}{\eta} \cdot |\,\boldsymbol{u} - \boldsymbol{v}\,|\,.$

The penality force term is modelled with the help of a step potential constant on the particles and zero outside.

3. Moving mesh definition

As already mentioned before, full Navier-Stokes equations have to be discussed in the model, because we will see that the magnetic forces acting on the particles lead to high velocities. Thus, in this particular model high local Reynolds numbers can be reached, though investigating a system on the microscale. It is therefore necessary to have an appropriate mesh resolution close to the particles themselves. As the particles move, the mesh has to be moved as well, which will be done in an ALE-framework.

Expecting the mesh velocity to equal the particle velocity on the particles and changing linearly in between, we come to a second domain triangulation, where the nodes are the particles, while the edges are the connections between certain neighboring beads (s. Fig. 1). Expecting the nodes of the triangle to be given by r_1, r_2 and r_3 with

$$r_i = (x_i, y_i)^T \qquad i = 1, 2, 3, \tag{3.1}$$

we can parameterize the triangles by parameters s_1 and s_2 by mapping the triangle onto the two dimensional simplex S_2. Using the affine mapping

$$\Phi_2(s_1, s_2) = r_1 + s_1(r_2 - r_1) + s_2(r_3 - r_1) \tag{3.2}$$

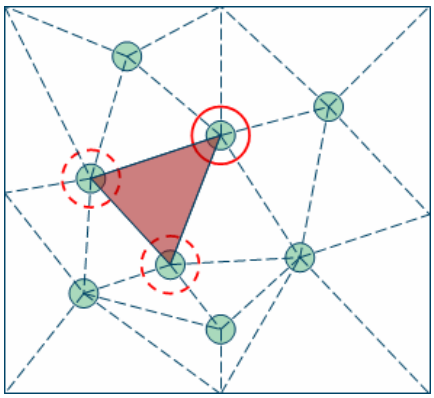

Fig. 1: Second domain triangulation defined by particle positions, the movement of the colored triangle is determined by the velocity of the particles in the corners. The triangulation itself is determined by Delaunay algorithm

it can be shown that

$$s_1 = \frac{(x-x_1)(y_3-y_1)-(x_3-x_1)(y-y_1)}{(x_2-x_1)(y_3-y_1)-(x_3-x_1)(y_2-y_1)}, \tag{3.3a}$$

$$s_2 = \frac{(x-x_1)(y_2-y_1)-(x_2-x_1)(y-y_1)}{(x_3-x_1)(y_2-y_1)-(x_2-x_1)(y_3-y_1)}. \tag{3.3b}$$

Suitable functions to model the mesh velocity as given below are thus given by the hat functions

$$\begin{aligned} d(x,y) &= 1-(s_1+s_2) \\ &= \frac{(y_3-y_2)(x_3-x)-(x_3-x_2)(y_3-y)}{(x_2-x_1)(y_3-y_1)-(x_3-x_1)(y_2-y_1)}. \end{aligned} \tag{3.4}$$

The functions d are 1 at x_1, 0 at x_2 and x_3 and linear in between (s. Fig. 2).

However, this choice leads to difficulties concerning numerical stability resulting from a strongly decreasing element quality of the original FEM-mesh. To overcome these problems slightly modified laws are applied:

$$\begin{aligned} f(d,\theta_1,\theta_2) = &\frac{d-\theta_1}{1-\theta_2-\theta_1}\cdot\Theta(d-\theta_1) \\ &\cdot\Theta(1-\theta_2-d)+\Theta(d-(1-\theta_2)) \end{aligned} \tag{3.5}$$

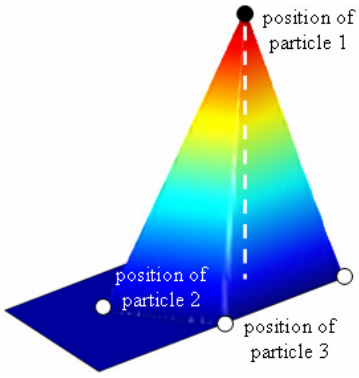

Fig. 2: Schematic drawing of the shape functions

where θ_1 and θ_2 are numerical parameters that will not discussed here in detail. The final expression describing the mesh displacement is given by summation over all nodes i. If the ALE-coordinates of a particle at spatial point r_i is given by ξ_i, the displacement Δr of an initial coordinate r may be written as

$$\Delta r = \sum_i (r_i - \xi_i)\cdot f(d_i(r),\theta_1,\theta_2). \tag{3.6}$$

Expression (3.6) is used for the mesh movement. Therefore, the ALE-application mode does not lead to any degrees of freedom to be solved for.

4. Simulation results

4.1 Particle behaviour

In our model situation, we expect superparamagnetic particles in a magnetic field rotating with a constant frequency f around the z-axis. As already mentioned before, a high spatial resolution is needed close to the particles. To achieve this we expect the particles to be point-like and choose the maximal element size at these points not to exceed 10^{-3} times the geometry size scale. The resulting mesh for a 2-particle case is shown in Fig. 3a. Dealing with point-like particles, the force density $\boldsymbol{f}$ in equation (2.5) goes over to a sum over point forces at position of the particles

$$\boldsymbol{f}(\boldsymbol{r},t) = \sum_i f_i(t)\cdot\delta(\boldsymbol{p}_i(t)-\boldsymbol{r}), \tag{4.1}$$

where $\boldsymbol{p}_i$ is the position of the i-th particle and $\boldsymbol{f}_i$ the density derived from (2.7). The force terms are implemented by additional weak point-terms.

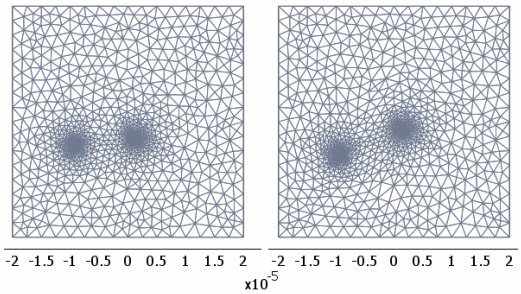

Fig. 3: Initial mesh and mesh at time $t = 10^{-4}s$

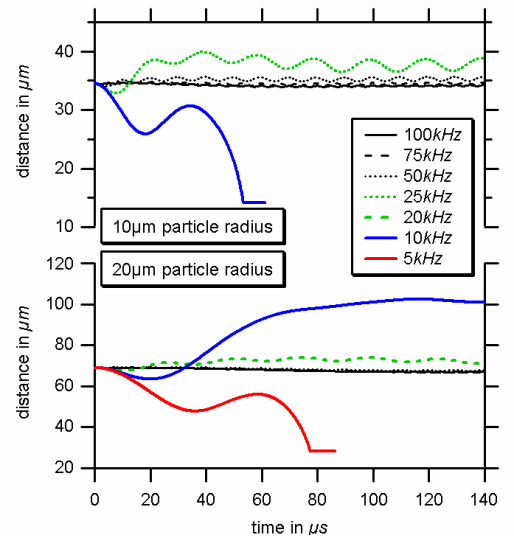

Fig. 4: Behaviour of the particle distance in respect to the field frequency for the case of a particle of radius a) $10\mu m$ and *b*) $20\mu m$

The calculations were carried under the assumption of a particle mass density of $2500 kg/m^3$ and a saturation magnetization of $1000 kA/m$. The carrier liquid is supposed to be water at room temperature, therefore, we expect a viscosity $\eta = 1.002 \cdot 10^{-3} Pa\ s$ and density $\rho_{flui} = 998.2 kg/m^3$. Starting with only two particles of radius r, we observe the following frequency dependent distance behaviour (Fig. 4): at low frequencies the distance of the particles strongly decreases and remains constant after a while. In this frequency area, the particles stick together and form rod-like agglomerations (Fig. 5) which also can be found experimentally. At very high frequencies particles oscillate against each other. However, due to a very rapidly changing magnetic field, the particles migrate close to their initial position. The average distance in respect to time a particle moves is close to zero. From Fig. 4 we learn that there is clearly a critical frequency

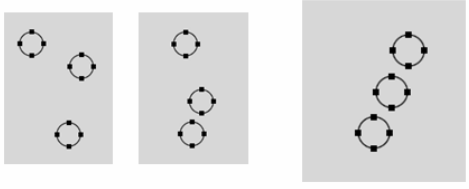

Fig. 5: Chain creation at low field frequencies

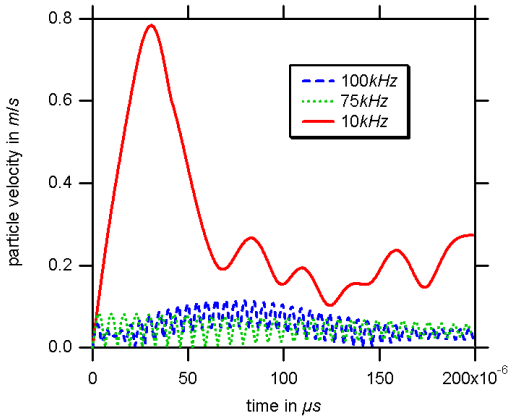

Fig. 6: Particle velocities for particle of radius $r = 10\mu m$ for different field frequencies

area, where the particles are pushed apart (~ $25 kHz$ for particles of radius $10\mu m$ and ~ $10 kHz$ for particles of radius $20\mu m$). This area changes, if particles of different size are investigated as can be seen in Fig. 4b. Similar results are obtained, if different values for the magnetization M_s are discussed.

Regarding the motion of the particles, it is interesting to notice that the particle on the microscale can actually reach macroscopic velocities (Fig. 6). Thus, it is not clear anymore, if magnetic or hydrodynamic interaction is the main force contribution at long distances.

4.2 Comparison between interactions

For the systems analyzed above, the two differrent force contributions are to be compared. In this case we expect two particles of a radius $r = 1\mu m$, whereas all other material parameters are chosen as above. The initial configuration equals the situation shown in Fig. 3. Applying a magnetic field of frequency $f = 50 kHz$ the particles oscillate close to their initial position inducing a velocity profile as shown in Fig. 7.

Expecting a third particle with radius a) r, b) $0.75r$ and c) $0.5r$ different degrees of importance of hydrodynamic and magnetic interactions can be found. Fig. 8 shows the areas where different forces are dominant. Blue areas correspond to magnetic, red to hydrodynamic contributions. A green coloring indicates the areas where both forces are of similar order. In all cases the hydrodynamic forces gain importance at long range.

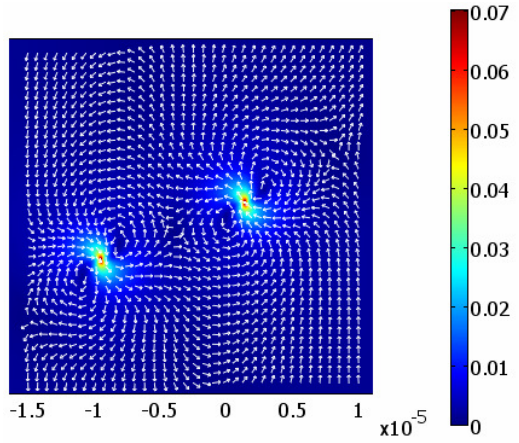

Fig. 7: Velocity profile resulting from particle movement at $t = 10^{-4}s$ for the parameters $r = 1\mu m$, $M_s = 1000kA/m$ and $f = 50kHz$

It is also remarkable that the hydrodynamic forces are independent of the saturation magnetization of the third particle. Therefore, hydrodynamic interactions even gain more importance, if particles of different magnetic moments are discussed.

5. Conclusions and Outlook

In the present work, we have shown that for magnetic particles in a rotational magnetic field not only the magnetic but also the hydrodynamic interactions are of importance.

Furthermore, the results obtained in the calculations indicate that the modeling of particles immersed in fluid flows with external magnetic fields as "free particles" might lead to wrong results, as even over distances of several times the particle diameter, strong magnetic as well as hydrodynamic interactions can be found.

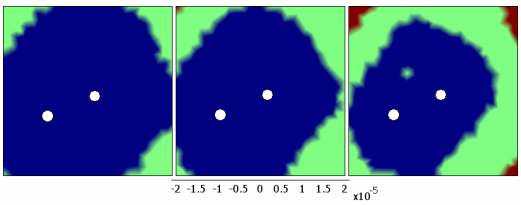

Fig. 8: Dominant force contribution plot, blue areas correspond to dominant magnetic forces, red to dominant fluidic contributions

6. References

[1] A. Grief, G. Richardson, Mathematical modelling of magnetically targeted drug delivery, J. Magn. Magn. Mater. **293** (2005) 455-463

[2] K. Smistrup, O. Hansen, H. Bruus, M. Hansen, Magnetic separation in microfluidic systems using microfabricated electromagnets – experiments and simulations, J. Magn. Magn. Mater. **293** (2005) 597-604

[3] J. Jackson, Classical Electrodynamics, Wiley, New York, 1999

[4] J. Coulson, J. Richardson, Chemical Engineering, vol. 2, Butterworth-Heinemann

7. Acknowledgements

The authors would like to thank the BMBF "MrBead"-project and the SFB 613 for financial support.